GEOCHRONOLOGY

EGU Open Access

Technical note: An analytical approach for (U–Th) / He dating of goethite by sample encapsulation in quartz ampoules under vacuum, with an example from the Amerasian Basin, Arctic Ocean

Olga Valentinovna Yakubovich[1,2], **Natalia Pavlovna Konstantinova**[2,3], **Maria Olegovna Anosova**[4], **Mary Markovna Podolskaya**[5], and **Elena Valerevna Adamskaya**[2]

[1]Department of Geochemistry, Saint Petersburg State University, St. Petersburg, 199034, Russia
[2]Laboratory of Isotope Geology, Institute of Precambrian Geology and Geochronology, RAS, St. Petersburg, 199034, Russia
[3]Institute for Geology and Mineral Resources of the Ocean (VNIIOkeangeologia), St. Petersburg, 190121, Russia
[4]Vernadsky Institute of Geochemistry and Analytical Chemistry, Moscow, 119991, Russia
[5]AnalyteMe, Reus, Tarragona, 43201, Spain

Correspondence: Olga Valentinovna Yakubovich (olya.v.yakubovich@gmail.com)

Abstract. We propose an analytical approach for (U–Th) / He dating of Fe-(oxyhydr)oxides that includes sealing samples in quartz ampoules and demonstrates its suitability as a reliable tool for the investigation of geological processes. The (U–Th) / He ages of goethite clasts and veins from Fe- and Mn-oxide cemented rocks recovered from the slope of the Chukchi Borderland in the Amerasia Basin demonstrate reproducibility, yielding a weighted mean age of 8.6 ± 0.3 Ma ($n = 4$) and 4.8 ± 0.4 Ma ($n = 2$), respectively, providing insights into the Neogene mineralization history of the region. This study also focuses on the sample preparation technique, which might influence the (U–Th) / He ages. Our data indicate that some of U can be leached from the goethite during sonication by distilled water, which might result in erroneous (U–Th) / He ages of multi-mineral grains. However, the analyzed goethite samples were formed in a specific underwater environment; so far it is not clear whether the same behavior of U would be observed in a terrestrial supergene goethite.

1 Introduction

The (U–Th) / He dating method is based on the α decay of U and Th that produce helium atoms. Traditionally, the ^{4}He isotopic systems have been successfully applied to low-temperature thermochronology (Farley and Stockli, 2002). Recent developments in understanding how helium behaves in various minerals have extended the method applicability in geochronological studies (Yakubovich et al., 2019; Shukolyukov et al., 2012a; Flowers et al., 2023, and references therein).

Fe-oxides and Fe-hydroxides, including goethite (α-FeO(OH)), lepidocrocite (γ-FeO(OH)), hematite (α-Fe$_2$O$_3$), maghemite (γ-Fe$_2$O$_3$) and magnetite (Fe^{2+}Fe$_2^{3+}$O$_4$), typically contain trace amounts of U and Th and therefore have been recognized as a potential geochronometer tool from the early days of geochronology (Strutt, 1908, 1909).

Goethite is one of the most common iron oxyhydroxide minerals formed during the hydrolyzation of rocks, making it a desirable mineral for dating various surface and subsurface geological processes. Helium diffusion studies (^{4}He/^{3}He spectra) revealed sufficient ^{4}He retentivity in goethite an the range of the near-surface temperatures, making the mineral suitable for (U–Th) / He weathering geochronology (Shuster et al., 2005). However, the accurate determination of He

diffusion parameters is complicated by the dehydration of goethite during vacuum step-heating experiments (Farley et al., 2023).

The (U–Th) / He dating of goethite was applied successfully in dating of weathering profiles (e.g., Monteiro et al., 2014; Riffel et al., 2016; Ansart et al., 2022), supergene ore formation (e.g., Vasconcelos et al., 2013; Heller et al., 2022; Verhaert et al., 2022) and diagenetic transformations (Reiners, 2014). The approach was also implemented successfully in dating deep-sea hydrothermal Fe-oxide mineralization (Benites et al., 2022). However, the dating of hydrogenetic Fe–Mn crusts is not robust due to the significant content of extraterrestrial He-rich dust and their high porosity, which prevent the accumulation of radiogenic He (Basu et al., 2006).

The (U–Th) / He dating of surface processes is challenging due to the multistage Fe-hydroxide formation. Several generations of the same phase intimately intergrow in a time span of millions of years (Vasconcelos et al., 2013; Monteiro et al., 2014; Heller et al., 2022). The presence of small inclusions of U- and Th-bearing contaminants may add difficulties to the interpretation of the isotopic results. Thus, high-resolution mineralogical and paragenetic characterization of the sample is required, which typically includes optical observations accompanied by XRD, SEM and chemical analyses (e.g., Monteiro et al., 2014; Hofmann et al., 2017; Deng et al., 2017).

From the analytical point of view, (U–Th) / He dating of goethite is challenging as well. The distribution of U and Th in the mineral is inhomogeneous (Shuster et al., 2005); therefore parental and daughter isotopes should be measured in the same sample. Helium release from the goethite must be carried out under strictly controlled laboratory heating conditions; otherwise, U and Th may be lost from the grains during He extraction, rendering the results inaccurate (Vasconcelos et al., 2013). There are several approaches to overcome this issue such as heating in the presence of oxygen (Hofmann et al., 2020) or using double-aliquot (Wernicke and Lippolt, 1993; Pidgeon et al., 2004) or multi-aliquot procedures (Wu et al., 2019). The last two require a remarkably larger amount of material.

Here, we propose an alternative (U–Th) / He dating methodology using an example of goethite from the Chukchi Borderland, Arctic Ocean. The technique was originally developed for the (U–Th) / He dating of native gold (Yakubovich et al., 2014) and pyrite (Yakubovich et al., 2020).

2   Samples

The Amerasia Basin of the Arctic Ocean remains one of the Earth's least explored region (Brumley et al., 2015). The Chukchi Borderland and Mendeleev Ridge are known as Paleozoic continental blocks that occur within the Amera-

sia Arctic Ocean. During US and Russian research cruises, fragments of Fe- and Mn-oxide mineralized rocks were collected from several sites of the northern Chukchi Borderland and central Mendeleev Ridge (Fig. 1a; (Hein et al., 2017; Konstantinova et al., 2017). The subject of this study is the age dating of samples from dredge haul DR7 collected from 3400 m water depth (coordinates 78.53° N, 156.68° W).

The DR7 dredge haul consists of rock fragments that are extensively altered and finely sheared. Two different rock types were found. The first one shows alternating yellow-brown and dark-brown layers, with dendrites of the dark-brown material in the yellow-brown laminae (Fig. 1b). Both layer types mainly comprise Fe-(hydro)oxides, but the dark-brown layers have a higher Mn-oxide content. Another rock type in DR7 is a breccia with poorly sorted predominantly angular to subangular clasts (Fig. 1c) that include pure Fe oxyhydroxide, basalt and altered metasedimentary rocks. Mn- or Fe-oxides are found in some larger clasts. The breccia cement is composed predominately of dark-brown Fe-oxyhydroxides with submetallic-gray areas. The microstructure varies from bladed to nodular to massive. The breccia is predominantly cement-supported, indicating replacement during Fe- and Mn-oxide mineralization. Thus, these samples do not represent the widespread underwater hydrogenic Fe–Mn mineralization (Hein et al., 2000). Their morphology, structure, mineral and chemical composition (especially high abundance of Fe-(hydro)oxides) indicate that they likely have a hydrothermal origin (Hein et al., 2024).

The dominant mineral in the mineralized samples based on X-ray diffractions is goethite and possibly lesser amounts of feroxyhyte (δ-FeOOH) and the ferrihydrite [$Fe^{3+}_{4-5}(OH,O)_{12}$] (Table 1; Fig. 2). The darker-colored goethite has better crystallinity than the paler ones.

Based on SEM–EDS studies (Fig. 3), Fe-oxide crystallite sizes of cement and replacements vary from a submicrometer to a few micrometers, rarely up to 120 μm. Birnessite and 10 Å manganates (todorokite, buserite or asbolane) and δ-MnO_2 (vernadite) occur as well. Relict host-rock minerals include quartz, feldspar, mica and clay minerals. Clinochlore (chlorite) is ubiquitous in the DR7 samples. Among the U-bearing minerals, single grains of zircon and monazite were observed (Fig. 3).

3   Methodology and sampling strategy

For (U–Th) / He dating fragments of goethite mineralization were manually extracted from the DR7-001 sample: dark-brown clasts of breccia and yellow-brown vein material (Fig. 1b). According to the SEM and XRD data, samples mainly consist of pure crystalline goethite (Figs. 2, 3) with a possible admixture of birnessite and quartz. Therefore, the samples represent a standard material which is used for (U–Th) / He dating. But samples themselves are not typical for (U–Th) / He studies. Most of the goethite grains that are used
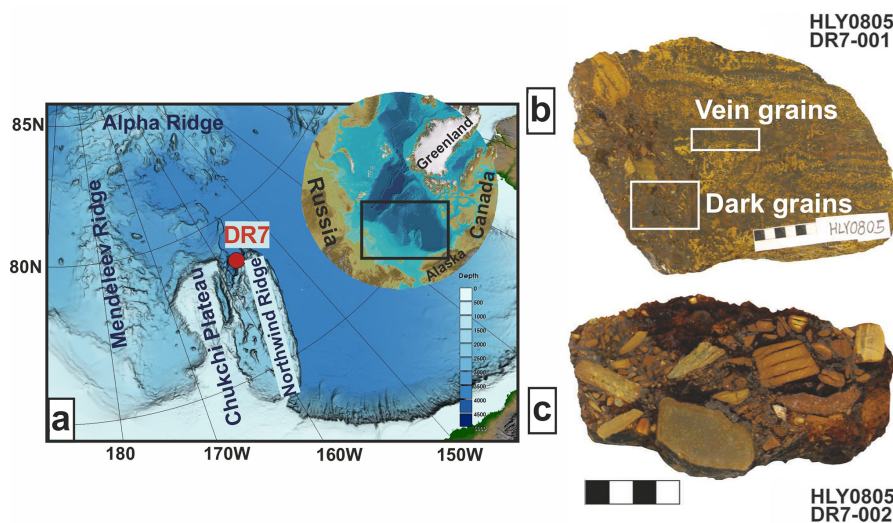
Figure 1. (a) Regional setting of the Amerasia Basin (inset) and location map of the DR7 dredge haul and **(b)** cut section images of the main sample types (modified from Hein et al., 2024). All subsamples for age dating are from DR7-001.

Table 1. XRD mineralogy of the crystalline phases of the DR7 sample from the Amerasia Arctic Ocean.

Sample ID	Description	Major	Moderate	Minor
DR7-001-L1A	Cement from breccia	Goethite	Quartz, birnessite	TAM
DR7-001-L1B	Glassy Fe-rich clast	Goethite	–	–
DR7-001-L2B	Fe-rich dark-brown lamina	Goethite, birnessite	Clinochlore, quartz, plagioclase	δ-MnO$_2$, TAM
DR7-001-L2D	Reddish vein	Goethite, quartz	Clinochlore, plagioclase, mica	Birnessite, TAM(?)
DR7-001-L2E	Fe–Mn lamina	Birnessite, goethite	TAM(?), quartz	Plagioclase

Major > 25 %, moderate 5 %–25 %, minor < 5 %. TAM is 10 Å manganates: todorokite, buserite or asbolane. Goethite may also include feroxyhyte or ferrihydrite (modified from Hein et al., 2024).
Comment: X-ray diffraction mineralogy was completed using a Malvern PANalytical X'Pert Powder X-ray diffractometer (XRD) with CuKα radiation and graphite monochromator run from 4 to 70° 2θ with a step size of 0.02° 2θ at 40 kV and 45 mA at USGS, PCMSC lab in 2017. Digital scans were analyzed using Philips X'Pert High Score Plus software to analyze X-ray reflections and identify possible mineral phases.

for He geochronology are from terrestrial supergene environment (Monteiro et al., 2024). The low-temperature steady and deep underwater environment ($\sim 0\,°C$) prevented thermal loss of He from the analyzed samples during their geological history.

3.1 Sample preparation

In order to exclude possible U loss during the sample preparation when goethite grains are sonicated in distilled water, leaching experiments were conducted. Millimeter-size fragments of goethite were manually extracted from the DR7-001 sample, which represented a dark-brown clast of the breccia and a yellow-brown vein material (Fig. 1b, c). In the first stage the massive single fragments in the closed Teflon vials with 3 mL of distilled deionized water (Barnstead) were sonicated for 15 min at room temperature (the temperature was not stabilized by extra cooling). The solution was removed by the mechanical pipette for subsequent chemical analysis. In the second stage the remained grains were dried at

room temperature for 24 h and crushed in the Teflon vial by the molybdenum stick ($< 300\,\mu m$) to increase their specific surface area. The crushed grains were sonicated in distilled deionized water (Barnstead; 3 mL) for extra 15 min at room temperature without extra cooling. After, the solutions were left for 24 h for the sinking of the small floating particles. The uppermost 1 mL of the solution was carefully moved to a new beaker, and nitric acid was added: up to 5 % HNO$_3$ solutions (50–150 μL). Uranium and Th contents were measured by an Element 2 ICP mass spectrometer at the Institute of Precambrian Geology and Geochronology, RAS. The full procedural blanks were obtained by the parallel procedures with an empty beaker. The total U and Th content of the sample was determined in the same way after its complete dissolution in the mixture of aqua regia (200 μL) with HF (250 μL) and HClO$_4$ (10 μL) for 15 h at 110 °C in a closed Teflon vial with a thermostat. Due to the described analytical procedure, the obtained U and Th contents in the leaching solutions are semi-quantitative.
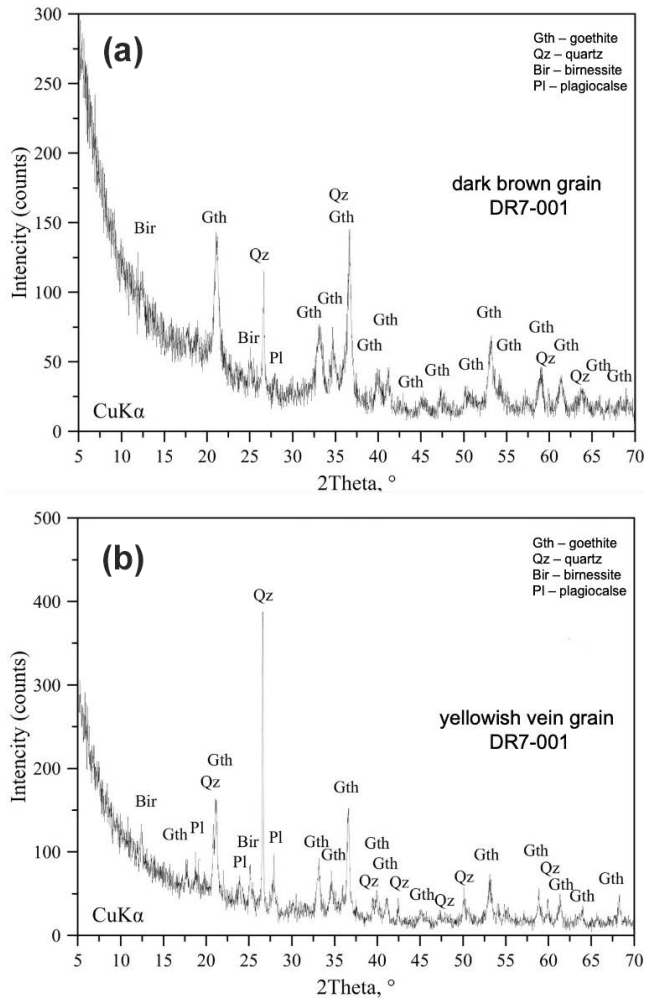
Figure 2. X-ray diffraction mineralogy of the dark-brown clast **(a)** and yellow-brown vein material **(b)** from the DR7-001 sample. Images modified from Hein et al. (2024).

3.2 (U–Th) / He dating

Eight millimeter-size fragments of goethite mineralization were manually extracted for (U–Th) / He dating from three different parts of the DR7-001 sample: two dark-brown clasts of the breccia and a yellow-brown vein from the completely altered rock (Fig. 1b, c; Table 2). Subsamples from the yellow-brown vein material and from dark-brown gains were treated as separate samples (1–8). Samples were derived from the inner part of the original sample, had no visible inclusions of other minerals under the binocular microscope and were not washed.

3.2.1 Measurement of radiogenic ^{4}He contents

For each measurement, $\sim$ 1–3 mg fragments of goethite grains were placed in a quartz ampoule ($\sim$ 1 cm long) and sealed under a 10^{-3} Torr vacuum (Fig. 4). The sealing was

Table 2. Results of (U–Th) / He dating of goethite subsamples of DR7-001.

No.	ID	Type	Mass [mg]	U [ppm]	U [10^{10} atoms]	σ [%]	Th [ppm]	Th [10^{10} atoms]	σ [%]	Th/U	^{4}He^d [cm^3 STP g^{-1}]	^{4}He [10^{10} atoms]	σ [%]	Age [Ma]	2σ
1	966	Dark grains	0.954	2.51	603	1.8	0.81	194	3.6	0.3	2.9×10^{-6}	7.54	2.3	9.1	0.5
2^a	969		7.197	1.86	3376	1.1	0.69	1258	2.1	0.4	3.4×10^{-6}	65.17	2.8	13.8	0.8
3	1015		1.946	2.62	1287	1.3	0.66	323	1.8	0.3	2.6×10^{-6}	13.73	3.7	7.9	0.6
4	1022		1.908	2.78	1338	1.8	0.81	387	2.0	0.3	3.1×10^{-6}	15.97	3.2	8.7	0.6
5^a	1031		2.973	2.43	1823	2.8	1.99	1491	2.4	0.8	4.3×10^{-6}	33.99	2.8	12.2	0.9
6	1032		3.115	2.25	1769	5.2	1.76	1379	5.0	0.8	2.6×10^{-6}	21.85	2.7	8.2	0.8
											Dark-brown grain weighted mean^c 8.6 ± 0.3				
7	1033	Vein grains	1.782	1.36	613	2.2	3.30	1481	1.6	2.4	1.1×10^{-6}	5.40	8.7	4.4	0.8
8	1036		2.708	1.80	1232	2.5	4.90	3347	1.9	2.7	1.8×10^{-6}	12.70	3.9	4.9	0.4
											Yellowish-brown vein weighted mean^c 4.8 ± 0.4				
Empty quartz ampoule^b			28–56	–	1.3	97	–	6	74	–	–	1.1	37	–	–

The reported uncertainties of U, Th and He measurements are the combined uncertainties calculated by summation in quadrature of measurement and blank uncertainties using a coverage factor of 1, which gives a level of confidence of approximately 65 %. ^{a} No. 2 and 5 ages not used in the calculation of mean age; see text in Results section for explanation. ^{b} Contents of U, Th and He in the quartz ampoule represent full analytical blank, which includes chemistry and steps of sample preparation (sealing, heating). ^{c} The reported uncertainties of an age value is an expanded analytical uncertainty, which includes analytical uncertainty of U, Th and He measurements and factors addressed in Sect. 4.2. Error value corresponds to 95 % level of confidence (2σ). ^{d} The calibration of the mass spectrometer was done using the mineral reference materials in a range of He content from 2 to 200 [10^{10} atoms].
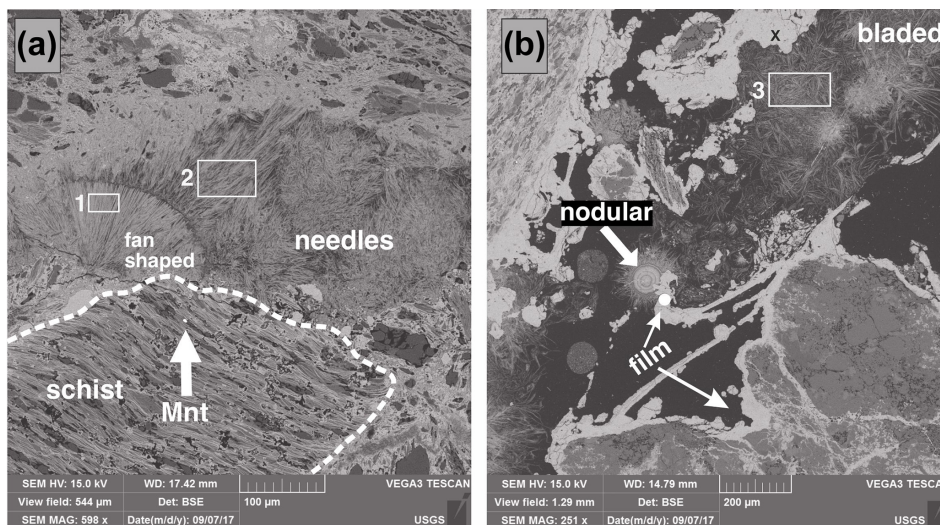
Figure 3. Backscatter SEM photomicrograph images of sample DR7-001 and DR7-002 from polished thin sections. **(a)** Fan-shaped (26 % Fe, 17 % Mn for box 1), needle (28 % Fe, 15 % Mn for box 2), and massive cement of Fe and Mn oxides in the breccia part of sample DR-001 (note the schist grain in the lower left quadrant with a bright monazite grain (Mnt)). **(b)** Cement of breccia: bladed (box 3: 29 % Fe, 35 % Mn), nodular (white arrow: 33 % Fe, 25 % Mn), and film type (white dot: 68 % Fe; black x: 35 % Fe, 29 % Mn) Fe- and Mn-oxide cement; bladed cement consists of discrete Mn-oxide and Fe-oxyhydroxide blades, and Fe and Mn contents vary for each laminae in the micronodule. Polished thin sections were carbon-coated and used for SEM–EDX analyses of samples DR7-001 and DR7-002 using a TESCAN VEGA3 scanning electron microscope (SEM) at operating conditions of 30 kV and 15 nA for imaging. The energy-dispersive spectroscopy (EDS) chemical characterization and element mapping were done using a JEOL 8900 operating at 15 kV and 40 nA for quantitative analyses of oxides. Counting times were 30 s peak and 15 s background at the USGS lab in Menlo Park in 2017.

done by the distilled water-based torch LIGA (Vasileostrovsky Electrochemical Plant). The torch has a narrow flame that prevents heating of the sample during the sealing. The Durango apatite ($n = 3$) sealed in a quartz ampoule by the same technique did not show any sign of He loss (Fig. S1 in the Supplement). The sealed ampoule, via a special gateway, was placed in a high-temperature high-vacuum furnace of the magnetic sector MSU-G-01-M mass spectrometer equipped with two SAES getter pumps (Spectron Analyt, IPGG, RAS; (Shukolyukov et al., 2012a, b). During heating, He easily diffuses through the thin quartz walls while U and other products of the sample decomposition remain in the ampoule. A Secondary Electron Multiplier (SEM) was used to determine the ^{4}He$^+$ beam intensity (cps). Calibration of the mass spectrometer was done using Knyahinya meteorite (Schultz and Franke, 2004) and RS-Pt reference material (Yakubovich et al., 2023).

Goethite samples were step-heated at temperatures of 350 °C for 30 min, 550 °C for 10 min, 900 °C for 10 min, 1100 °C for 15 min and 1150 °C until He stopped being released (5 min in average). Samples 1 and 2 (ID 966, 969, Table 2) were step-heated under slightly different conditions, starting with a temperature of 240 °C. This step-heating approach allows for monitoring the He release pattern from the goethite grains as well as the excess hydrogen (ion HD$^+$) in the chamber of the mass spectrometer. The diffusion of He through the thin quartz walls of the ampoule is fast (Shuster

and Farley, 2005; Yakubovich et al., 2014), but it does not allow one to obtain the accurate diffusion kinetics of He from the goethite grains.

Following the extraction of He, the ampoule was removed from the mass spectrometer for subsequent separation of U and Th.

The total procedural blank, determined by heating the empty quartz ampoules to 1100 °C, corresponds to $4.4 \pm 1.6 \times 10^{-10}$ cm^3 He at STP.

3.2.2 Measurement of U and Th contents

The quartz ampoule with degassed samples was spiked with a ^{230}Th–^{235}U tracer and dissolved in a mixture of aqua regia (0.4 mL), concentrated hydrofluoric acid (0.5 mL) and perchloric acid (0.05 mL) in closed Teflon vials for 2 h at 200 °C on a hot plate followed by 15 h at 110 °C in a thermostat. The solution was dried on a hot plate at 200 °C. During this step, perchloric acid prevented the formation of low-soluble fluorine complexes, while most of Si evaporated in a form of SiF$_4$. The remaining precipitate was dissolved in 1.5 mL of 5 % nitric acid and heated up to 80 °C in an ultrasonic bath for 15 min prior the measurement of U and Th contents. ^{235}U/^{238}U and ^{230}Th/^{232}Th isotope ratios were measured on an Element XR ICP mass spectrometer at the Vernadsky Institute of Geochemistry and Analytical Chemistry, RAS. The total chemical procedure blank, determined by dissolution of
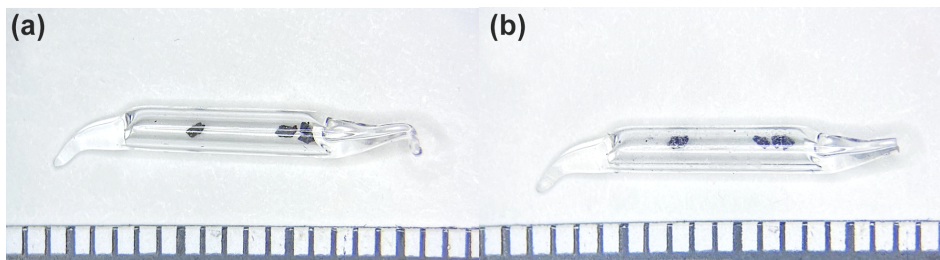
Figure 4. Fragments of goethite in a sealed quartz ampoule **(a)** before heating and **(b)** after heating. Scale bar: 1 mm.

the empty quartz ampoules ($n = 4$) using the same settings, corresponds to 1.30 ± 1.26 and $5.8 \pm 4.4 \; 10^{10}$ atoms of ^{238}U and ^{232}Th respectively.

The (U–Th) / He ages were calculated using IsoplotR software (Vermeesch, 2018). The combined analytical uncertainty was estimated based on the U, Th and He measurement uncertainties and the uncertainty based on the blank determinations. The α-recoil corrections were not applied, because all analyzed samples are the fragments of large grains.

4 Results

4.1 Leaching experiments

Chemical analyses of the distilled water leachates revealed the partial loss of U and Th from the subsamples (Table 3). The leaching of U and Th from the crushed subsample is more intensive than from a massive grain and reaches up to 8 % for U and less than 2 % for Th. Because the samples are not water-soluble but the leachates contain also some amount of Mn, Fe and Co, some tiny floating particles of the original sample might be in the solution. The ICP-MS measurements were calibrated only for U and Th, thus determining that the concentration of Mn and Fe in the solutions was not possible. However, the notable shift of the Th/U ratio in the solution relative to the Th/U ratio of the residual goethite (from 0.06 to 3; Table 3) indicates that some part of U was leached from the samples. These findings are in an agreement with previous results of Fe- and Mn-oxides leaching experiments by a weak acids with an acetate buffer (Konstantinova et al., 2018; Koschinsky and Hein, 2003), which implies U- and Th-adsorbed behavior.

4.2 (U–Th) / He dating results

The (U–Th) / He ages for eight fragments of goethite from sample DR-7-001 included fragments of two sets of dark grains from two separate breccia goethite clasts (grains 1–4 and 5–6) and one set of yellow-brown vein samples (grains 7–8) (Table 2; Fig. 5). The signals of He, U and Th of all samples were markedly higher than the background level (empty quartz ampoule). The concentrations of U in the dark goethite grains range from 2.2–2.8 ppm, with Th/U ratios of

0.3–0.8. The concentration of U in the two vein subsamples is lower (1.36 and 1.8 ppm), and Th prevails over U (Th/U 2.4–2.7). Concentrations of ^{4}He range from 2.6 to $4.3 \times 10^{-6} \; \mathrm{cm^3 \; STP \; g^{-1}}$ for the dark-brown grains and from 1.1 to $1.8 \times 10^{-6} \; \mathrm{cm^3 \; STP \; g^{-1}}$ for vein samples. Among the six dark goethite grains analyzed, one had an atypically low U concentration (1.86 ppm; Table 2). Sample 5 (ID 1031) had an unusual high-temperature He release pattern ($> 1100°$, Fig. 7), which likely indicates the presence of He-retentive mineral inclusions. These anomalous samples (ID 969; 1031) revealed (U–Th) / He age in a range of 12.2–13.8 Ma (Table 2). The coincidence of their (U–Th) / He ages might indicate that we were wrong when we decided to exclude these grains from consideration. However, in a lack of confidence we are not going to interpret this age value.

The (U–Th) / He age of the remaining dark grains is consistent within the uncertainty of the measurements with a weighted mean value of 8.6 ± 0.3 Ma (2σ). The two yellow-brown vein samples had significantly younger reproducible ages, with a mean of 4.8 ± 0.4 Ma (2σ).

5 Discussion

5.1 Methodological implications

5.1.1 Sample preparation

Due to the leaching experiments, around 8 % of U and 1.7 % of Th can be remobilized from the sample by the freshly deionized distilled water, which is known to became chemically active after contact with the atmosphere (pH 5–6; Gurr, 1962). Goethite is not a water-soluble mineral. Therefore, U release likely indicates its position beyond the crystal lattice or in some unstable phases. Th/U ratios of the grains (0.3 and 1.3 for dark grains, 2.5 and 3.0 for a vein material) are remarkably higher than those of leachates (0.06 and 0.6 for dark grains and 0.6 and 1.7 for vein material; Table 3), which implies that U is easier to mobilize. This is in favor of the adsorbed form of some of the U, rather than the presence of unstable phases with different Th/U ratios. The higher percent of U loss from the crushed samples is also in agreement with this suggestion (Table 3).

Table 3. Results of the leaching experiments of goethite subsamples of DR7-001.

Sample	Stage	Weight, mg	U, ng	Th, ng	Th/U	Fraction of U loss	Fraction of Th loss
Dark grain	first	5.628	0.03	0.01	0.26	0.3	0.3
	second		0.38	0.02	0.06	3.5	0.6
	residual		10.7	3.4	0.32	–	–
Dark grain-2*	second	2.462	0.03	0.02	0.6	0.5	0.23
	residual		5.4	7.3	1.3		
Vein grain	first	6.212	0.01	0.02	1.4	0.12	0.10
	second		0.6	0.40	0.6	7.8	1.6
	total		8.4	24.7	2.5	–	–
Vein grain-2*	second	1.890	0.11	0.19	1.7	3.0	1.7
	residual		3.6	10.9	3.0		
Blank	first	–	0.004	0.002	0.5	–	–
	second	–	0.01	0.005	0.7	–	–
	residual	–	0.01	0.02	1.8	–	–

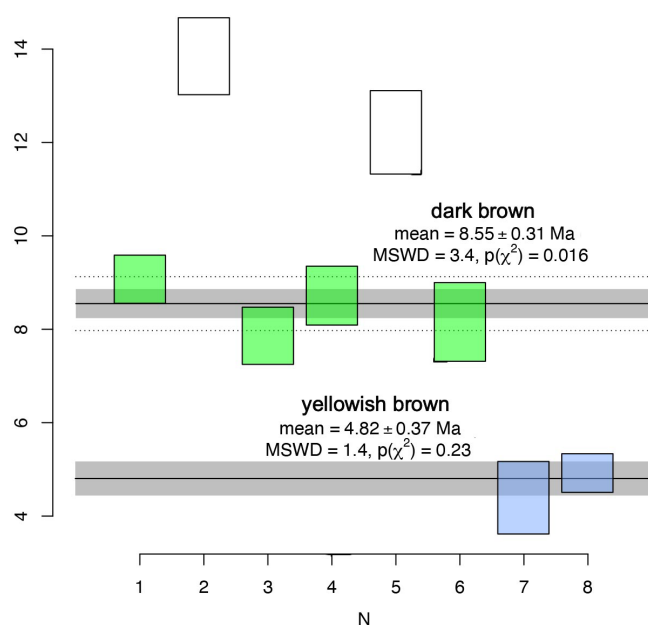* Grains were crushed and sonicated without a prior step (first stage).

Figure 5. Results of (U–Th) / He dating of goethite from DR7-001 subsamples. Error bars are 2σ. Weighted mean plot constructed using IsoplotR software (Vermeesch, 2018).

The possible adsorbed behavior of U in goethite from the weathering environment was discussed by Shuster et al. (2005) and Vasconcelos et al. (2013). The leaching experiments are also in agreement with the results of radiochemical experiments that revealed that during the crystallization of hematite and goethite from ferrihydrite $(Fe^{3+})_2O_3 \cdot 0.5H_2O$, which is the least stable iron (oxyhydr)oxide, only part of uranium becomes leaching-resistant (Payne et al., 1994).

The proportion of U in adsorbed form relative to the U, which is incorporated into crystal lattice, can differ from sample to sample. This is indirectly confirmed by the discussion in Vasconcelos et al. (2013), who suggest that various patterns of U loss during the He release from the goethite samples possibly indicated a different U position of the analyzed samples. Adsorbed behavior of some of the U does not strongly affect the applicability of the (U–Th) / He method due to the long α-stopping distances (Shuster et al., 2005). However, sonication of the samples in distilled water prior to (U–Th) / He dating might result in U loss and subsequent erroneous and/or over-dispersed ages of multi-mineral grains. Large grains (crystals > 50–$70\,\mu m$) are unlikely to lose a significant amount of U as their surface-to-volume ratio is low.

5.1.2 Justification of the technique

(U–Th) / He ages of goethite subsamples are reproducible. Measured concentrations of U in the samples that were degassed in the quartz ampoules (1.4–2.8 ppm; Table 2) are in the range of their concentrations in the unheated grains (1.5–2.5 ppm; $n = 5$; ICP MS). This indicates that the proposed analytical approach is well suited for (U–Th) / He dating of goethite and likely other Fe-oxyhydroxides. Encapsulating the individual goethite grains into the quartz ampoule excludes any U loss during the sample degassing, which is one of the major analytical concerns (Vasconcelos et al., 2013; Hofmann et al., 2020; Wu et al., 2019). The approach allows overheating of the sample with plenty of reserve. Based on our experience with He release from isoferroplatinum (Pt_3Fe), quartz ampoules are robust in temperatures up to $1450\,°C$ (Shukolyukov et al., 2012b). One of the main disadvantages of the proposed technique is the relatively high blank of the quartz ampoule, which complicates analysis

of grains that are very small and/or too young. The technique is quite sufficient for (U–Th) / He dating of milligram-weighted samples of Neogene age as tested here and requires a remarkably lower amount of the material than double- or multi-aliquot approaches (Pidgeon et al., 2004; Wu et al., 2019). The technique also does not require the modernization of the He extraction line, which is needed for degassing in the presence of O_2 (Hofmann et al., 2020).

5.1.3 Future developments

In order to determine the analytical limitations of the proposed methodological approach, additional tests and improvements should be done in the future. The technique is based on several key assumptions. The first assumption (a) is that no He loss occurs from the sample when sealing a quartz ampoule with a torch. Several experiments support this assumption, conducted on Durango apatite (Fig. S1) and more He-retentive minerals such as isoferroplatinum (Yakubovich, 2013) and pyrite (Yakubovich et al., 2020). However, it would be necessary to date Fe-oxyhydroxides with this technique with independent age constraints in order to confirm the suitability of the procedure. Measurement of a comprehensive set of Durango apatite grains with the same approach is another possible way to confirm the absence of He lost by the grains during the sealing procedure.

The second assumption (b) is that heating at 1150 °C is sufficient to release all He from the goethite grains. This is based on the observed He release pattern, but further verification is needed. Future experiments should involve heating goethite to higher temperatures to confirm the complete release of He.

The third assumption (c) is that the quartz ampoule prevents U loss. This is based on the relatively slow diffusion of uranium (U) in quartz. However, to validate this, it is necessary to compare the results with U and Th measurements from unheated aliquots to demonstrate complete recovery of volatilized U. Since goethite is opaque, and mineral inclusions could affect (U–Th) / He ages, pre-screening the grains using micro-CT would be important for these tests and would enhance the proposed methodological approach.

This study also identified that U can leach from goethite during sonication in distilled water. The hypothesis of U mobilization from goethite is primarily based on the shift in the Th/U ratio in the solution compared to the residual goethite (Table 3). However, this observation is indirect, as other factors, such as intrinsic variability in the Th/U ratio of the goethite, may contribute to this shift. To confirm U mobilization, a series of experiments comparing the (U–Th) / He ages of washed and unwashed goethite grains is necessary. It remains unclear whether this U behavior is specific to underwater hydrothermal multi-mineral goethite or whether a similar pattern could be observed in terrestrial supergene goethite.
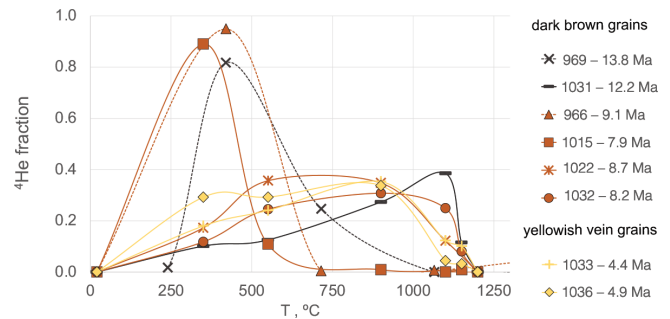

Figure 6. Helium release pattern from the mainly (> 95 %) goethite grains sealed in quartz ampoules. All measurements (with the exception of samples 966 and 969; dotted line) were carried out under the same time–temperature conditions. Values are the sample IDs in Table 2.

5.2 Geological implications

The results of the (U–Th) / He age dating of goethite grains from the slope of the Chukchi Borderland produce a Neogene age formation. There are several factors that might potentially affect the mineral age results, such as He loss, radiation damage, recrystallization, and fluid and mineral inclusions, which we discuss below.

5.2.1 Helium thermal retentivity

Goethite is predominantly He-retentive under surface conditions (Cooperdock and Ault, 2020). The mineral is able to retain around 80 %–95 % of its radiogenic ^{4}He for millions of years (Shuster et al., 2005; Deng et al., 2017; Hofmann et al., 2017). The water temperature at 3400 m water depth within the Chukchi Borderland slope is about −0.3 °C (Zhang et al., 2021). Therefore, any thermal loss of He seems unlikely, though it could be induced by local hydrothermal events.

Heating the sample in a quartz ampoule does not allow the measurement of the He diffusion parameters. Nevertheless, it does reflect the He retentivity of the sample. Despite different He release patterns (Fig. 6) the (U–Th) / He age of the same group is quite uniform, which likely indicates insignificant thermal loss of ^{4}He (Fig. 6). What is remarkable is that the He release pattern of sample 3 (ID 1015) significantly differs from the patterns of the other grains, despite its (U–Th) / He age being consistent with other measurements.

5.2.2 Radiation damage

The He diffusivity of a mineral can be strongly affected by the amount of accumulated radiation damage (Flowers et al., 2023). The standard technique that is used to investigate the role of radiation damage and elemental substitution is not applicable to goethite due to its dehydration during vacuum step heating (Farley et al., 2023). Numerical simulations, which combined the density functional theory (DFT) and kinetic Monte Carlo (KMC) simulations, predict that He loss from
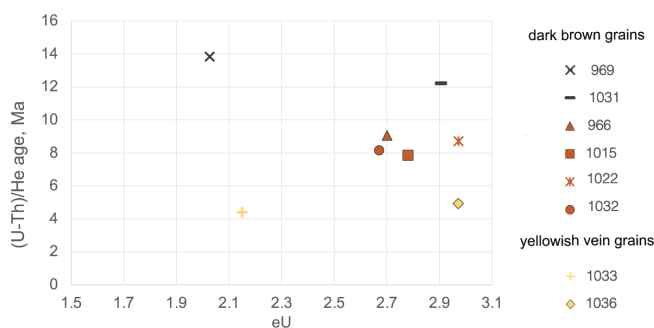
Figure 7. Goethite (U–Th) / He ages versus eU concentration of the samples. The effective modern uranium concentration (eU) was calculated based on the formulas given by Flowers et al. (2023). Index is the sample ID in Table 2.

goethite is strongly controlled by radiation damage and some other impurities (e.g., Al) (Bassal et al., 2022).

The samples have close values of eU content, and in the limited range of its variation there is no correlation with (U–Th) / He age values (Fig. 7). The uniform (U–Th) / He ages of the petrological groups (clasts and vein) indicate limited impact of the radiation damage on the dispersion of He ages.

5.2.3 Mineral and fluid inclusions and impurities

The studied samples contain rare U- and Th-rich mineral inclusions, such as zircon and monazite, with sizes ranging between < 1 and $40\,\mu m$ (e.g., Fig. 3). If there were incomplete dissolution within the chemical procedure, the U-loss would result in erroneously old and unreproducible ages, which might be the case of sample 5 (ID 1031).

Helium concentration of mineral fluid inclusions that formed during magmatic and hydrothermal processes typically does not exceed $10^{-8}\,cm^3\,STP\,g^{-1}$ (Stuart et al., 1994; Graupner et al., 2006), which is less than 1 % of the total He of the studied samples and insignificant for our (U–Th) / He dating procedure.

Incorporation of Sm can be an additional source of ^{4}He in goethite. Sm contents of the DR7-001 samples vary from 5.5 to 6 ppm (ICP-MS data; lithium metaborate fused disks; $n = 3$), which implies that Sm would produce less than 0.25 % of the He sample budget.

XRD data indicate that goethite from yellow-brown vein material has lower crystallinity and a higher abundance of mineral inclusions such as quartz, plagioclase and illite (Fig. 2; Table 1). These factors might potentially decrease the (U–Th) / He age of the samples. Thus, we cannot exclude that the younger age of goethite from the yellow-brown vein is related to some He loss.

5.2.4 Recrystallization

Goethite is the most thermodynamically stable Fe-oxyhydroxide in the near-surface environment. However, it can undergo dissolution–recrystallization processes during interaction with acidic solutions that reset its (U–Th) / He age (Monteiro et al., 2014). These processes enrich samples with low-soluble components that increase the Th/U ratios. This might be initiated by the presence of Fe^{2+} ions in aquatic systems (Handler et al., 2014). Given that the vein has higher Th/U ratios (2.5–2.7 vs. 0.3–0.8 of the dark grains) and younger (U–Th) / He age ($4.8 \pm 0.9\,Ma$ vs. $8.6 \pm 1.2\,Ma$; Table 2), its new formation due to the recrystallization of goethite cannot be ruled out.

5.2.5 Interpretation of (U–Th) / He ages

In addition to assessment of the all factors that might impact the (U–Th) / He ages, we include 10 % (2σ) uncertainty to the primary analytical uncertainty of the measurements based on the suggestion of Monteiro et al. (2014). Thus, the dense dark-brown goethite has an age of $8.6 \pm 1.2\,Ma$ (2σ), and the vein material is younger, $4.8 \pm 0.9\,Ma$ (2σ). These values do not overlap within the extended uncertainty.

The (U–Th) / He ages reflect the time of mineral formation, recrystallization or cooling below the closure temperature. Closure temperature of goethite varies over a wide range, from ~ 20 to $150\,°C$, depending on the diffusion domain sizes and distribution of the defects in the crystal lattice (Bassal et al., 2022). Thus, the uniform (U–Th) / He ages of the dark-brown grains accompanied by remarkably different He release patterns (Fig. 6) might be explained by cooling, only with the assumption of fast (1–2 Myr) host rock uplift from ~ 2–4 km depth that took place at $\sim 9\,Ma$. However, that assumption is inconsistent with the tectonic evolution of the Arctic region (e.g., (Chian et al., 2016; Craddock and Houseknecht, 2016). Therefore, (U–Th) / He ages of the dark grains of pure crystalline goethite reflect a Neogene mineralization event in the Chukchi Borderland, Arctic Ocean. More data are required in order to check the possible presence of fragments of older Fe- and Mn-mineralized rocks (12–14 Ma; Table 2), as well as to confirm the young ($\sim 4.8\,Ma$) mineralization event.

6 Conclusions

Reproducible (U–Th) / He ages are achieved using our proposed analytical approach, which involves sealing the sample in a quartz ampoule for He release, which is well suited for (U–Th) / He dating of Fe-oxyhydroxides; this technique allows for the determination of U, Th and He on the same subsample aliquot. Our data also indicate a fraction of U can be leached from multi-grain goethite samples during sonication in distilled water, implying that this step of goethite

sample preparation for (U–Th) / He dating should be taken with caution.

(U–Th) / He ages of goethite from the slope of the Chukchi Borderland formed during a Neogene mineralization event (8.6 ± 1.2 Ma). The younger age of the yellow-brown vein material (4.8 ± 0.9 Ma) can be explained by an episode of later-stage mineralization, recrystallization or by its lower crystallinity. Further investigations and a larger sample set are recommended for a comprehensive understanding of the geological evolution of the region.

Data availability. All data supporting the findings of this study are included within the manuscript as tables and graphs. No additional datasets were generated or analyzed during this study. Readers are encouraged to contact the corresponding author for any further inquiries or clarification regarding the presented data.

Supplement. The supplement related to this article is available online at: https://doi.org/10.5194/gchron-6-653-2024-supplement.

Author contributions. OY and NK: conceptualization, writing (review and editing), project administration. OY, NK, MA, MP and EA: formal analysis, investigation, methodology.

Competing interests. The contact author has declared that none of the authors has any competing interests.

Disclaimer. Publisher's note: Copernicus Publications remains neutral with regard to jurisdictional claims made in the text, published maps, institutional affiliations, or any other geographical representation in this paper. While Copernicus Publications makes every effort to include appropriate place names, the final responsibility lies with the authors.

References

Ansart, C., Quantin, C., Calmels, D., Allard, T., Roig, J. Y., Coueffe, R., Heller, B., Pinna-Jamme, R., Nouet, J., Reguer, S., Vantelon, D., and Gautheron, C.: (U-Th) / He Geochronology Constraints on Lateritic Duricrust Formation on the Guiana Shield, Front. Earth Sci., 10, 1–19, https://doi.org/10.3389/feart.2022.888993, 2022.

Bassal, F., Heller, B., Roques, J., Balout, H., Tassan-Got, L., Allard, T., and Gautheron, C.: Revealing the radiation damage and Al-content impacts on He diffusion in goethite, Chem. Geol., 611, 121118, https://doi.org/10.1016/j.chemgeo.2022.121118, 2022.

Basu, S., Stuart, F. M., Klemm, V., Korschinek, G., Knie, K., and Hein, J. R.: Helium isotopes in ferromanganese crusts from the central Pacific Ocean, Geochim. Cosmochim. Ac., 70, 3996–4006, https://doi.org/10.1016/j.gca.2006.05.015, 2006.

Benites, M., Hein, J. R., Mizell, K., Farley, K. A., Treffkorn, J., and Jovane, L.: Geochemical insights into formation of enigmatic ironstones from Rio Grande rise, South Atlantic Ocean, Mar. Geol., 444, 106716, https://doi.org/10.1016/j.margeo.2021.106716, 2022.

Brumley, K., Miller, E. L., Konstantinou, A., Grove, M., Meisling, K. E., and Mayer, L. A.: First bedrock samples dredged from submarine outcrops in the Chukchi Borderland, Arctic Ocean, Geosphere, 11, 76–92, https://doi.org/10.1130/GES01044.1, 2015.

Chian, D., Jackson, H. R., Hutchinson, D. R., Shimeld, J. W., Oakey, G. N., Lebedeva-Ivanova, N., Li, Q., Saltus, R. W., and Mosher, D. C.: Distribution of crustal types in Canada Basin, Arctic Ocean, Tectonophysics, 691, 8–30, https://doi.org/10.1016/j.tecto.2016.01.038, 2016.

Cooperdock, E. H. G. and Ault, A. K.: Iron oxide (U-Th)/he thermochronology: New perspectives on faults, fluids, and heat, Elements, 16, 319–324, https://doi.org/10.2138/gselements.16.5.319, 2020.

Craddock, W. H. and Houseknecht, D. W.: Cretaceous-Cenozoic burial and exhumation history of the Chukchi shelf, offshore Arctic Alaska, Am. Assoc. Pet. Geol. Bull., 100, 63–100, https://doi.org/10.1306/09291515010, 2016.

Deng, X. D., Li, J. W., and Shuster, D. L.: Late Mio-Pliocene chemical weathering of the Yulong porphyry Cu deposit in the eastern Tibetan Plateau constrained by goethite (U–Th)/He dating: Implication for Asian summer monsoon, Earth Planet. Sc. Lett., 472, 289–298, https://doi.org/10.1016/j.epsl.2017.04.043, 2017.

Farley, K. A. and Stockli, D. F.: (U-Th) / He Dating of Phosphates: Apatite, Monazite, and Xenotime, Rev. Mineral. Geochem., 48, 559–577, https://doi.org/10.2138/rmg.2002.48.15, 2002.

Farley, K. A., Monteiro, H. B., Vasconcelos, P. M., and Waltenberg, K.: Dehydration of goethite during vacuum step-heating and implications for He retentivity characterization, Chem. Geol., 663, 122254, https://doi.org/10.1016/j.chemgeo.2024.122254, 2023.

Flowers, R. M., Zeitler, P. K., Danišík, M., Reiners, P. W., Gautheron, C., Ketcham, R. A., Metcalf, J. R., Stockli, D. F., Enkelmann, E., and Brown, R. W.: (U-Th) / He chronology: Part 1. Data, uncertainty, and reporting, Bull. Geol. Soc. Am., 135, 104–136, https://doi.org/10.1130/B36266.1, 2023.

Graupner, T., Niedermann, S., Kempe, U., Klemd, R., and Bechtel, A.: Origin of ore fluids in the Muruntau gold system: Constraints from noble gas, carbon isotope and halogen data, Geochim. Cosmochim. Ac., 70, 5356–5370, https://doi.org/10.1016/j.gca.2006.08.013, 2006.

Gurr, E.: Effect of heat on the pH of water and aqueous dye solutions, Nature, 4847, 1199–1200, 1962.

Handler, R. M., Frierdich, A. J., Johnson, C. M., Rosso, K. M., Beard, B. L., Wang, C., Latta, D. E., Neumann, A., Pasakarnis, T., Premaratne, W. A. P. J., and Scherer, M. M.: Fe(II)-catalyzed recrystallization of goethite revisited, Environ. Sci. Technol., 48, 11302–11311, https://doi.org/10.1021/es503084u, 2014.

Hein, J. R., Konstantinova, N., Mikesell, M., Mizell, K., Fitzsimmons, J. N., Lam, P. J., Jensen, L. T., Xiang, Y., Gartman, A., Cherkashov, G., Hutchinson, D. R., and Till, C. P.: Arctic Deep Water Ferromanganese-Oxide Deposits Reflect the Unique Characteristics of the Arctic Ocean, Geochem. Geophys. Geosy., 18, 3771–3800, https://doi.org/10.1002/2017GC007186, 2017.

Hein, J. R., Koschinsky, A., Bau, M., Manheim, F. T., Kang, J.-K., and Roberts, L.: Cobalt-rich ferromanganese crusts in the Pacific, in: Handbook of marine mineral deposits, edited by: Cronan, D. S., 239–279, ISBN 0-8493-8429-X, 2020.

Hein, J. R., Mizell, K., and Gartman, A.: Neogene hydrothermal Fe- and Mn-oxide mineralization of Paleozoic continental rocks, Amerasia Basin, Arctic Ocean, Geochem. Geophy. Geosy., 25, e2023GC010996, https://doi.org/10.1029/2023GC010996, 2024.

Heller, B. M., Riffel, S. B., Allard, T., Morin, G., Roig, J. Y., Couëffé, R., Aertgeerts, G., Derycke, A., Ansart, C., Pinna-Jamme, R., and Gautheron, C.: Reading the climate signals hidden in bauxite, Geochim. Cosmochim. Ac., 323, 40–73, https://doi.org/10.1016/j.gca.2022.02.017, 2022.

Hofmann, F., Reichenbacher, B., and Farley, K. A.: Evidence for > 5 Ma paleo-exposure of an Eocene–Miocene paleosol of the Bohnerz Formation, Switzerland, Earth Planet. Sc. Lett., 465, 168–175, https://doi.org/10.1016/j.epsl.2017.02.042, 2017.

Hofmann, F., Treffkorn, J., and Farley, K. A.: U-loss associated with laser-heating of hematite and goethite in vacuum during (U–Th)/He dating and prevention using high O$_2$ partial pressure, Chem. Geol., 532, 119350, https://doi.org/10.1016/j.chemgeo.2019.119350, 2020.

Konstantinova, N., Cherkashov, G., Hein, J. R., Mirão, J., Dias, L., Madureira, P., Kuznetsov, V., and Maksimov, F.: Composition and characteristics of the ferromanganese crusts from the western Arctic Ocean, Ore Geol. Rev., 87, 88–99, https://doi.org/10.1016/j.oregeorev.2016.09.011, 2017.

Konstantinova, N., Hein, J. R., Gartman, A., Mizell, K., Barrulas, P., Cherkashov, G., Mikhailik, P., and Khanchuk, A.: Mineral phase-element associations based on sequential leaching of ferromanganese crusts, Amerasia Basin Arctic ocean, Minerals, 8, 460, https://doi.org/10.3390/min8100460, 2018.

Koschinsky, A. and Hein, J. R.: Uptake of elements from seawater by ferromanganese crusts: Solid-phase associations and seawater speciation, Mar. Geol., 198, 331–351, https://doi.org/10.1016/S0025-3227(03)00122-1, 2003.

Monteiro, H. S., Vasconcelos, P. M., Farley, K. A., Spier, C. A., and Mello, C. L.: (U-Th) / He geochronology of goethite and the origin and evolution of cangas, Geochim. Cosmochim. Ac., 131, 267–289, https://doi.org/10.1016/j.gca.2014.01.036, 2014.

Monteiro, H. S., Farley, K. A., and Vasconcelos, P. M.: Short Communication: A database of the global distribution of (U-Th)/He ages and U, Th contents of goethites, Geochronology Discuss. [preprint], https://doi.org/10.5194/gchron-2024-13, in review, 2024.

Payne, T. E., Davis, J. A., and Waite, T. D.: Uranium Retention by Weathered Schists – The Role of Iron Minerals, Radiochim. Acta, 66–67, 297–304, https://doi.org/10.1524/ract.1994.6667.special-issue.297, 1994.

Pidgeon, R. T., Brander, T., and Lippolt, H. J.: Late Miocene (U+Th)-4He ages of ferruginous nodules from lateritic duricrust, Darling Range, Western Australia, Aust. J. Earth Sci., 51, 901–909, https://doi.org/10.1111/j.1400-0952.2004.01094.x, 2004.

Reiners, P. W., Chan, M. A., and Evenson, N. S.: (U-Th) / He geochronology and chemical compositions of diagenetic cement, concretions, and fracture-filling oxide minerals in mesozoic sandstones of the Colorado Plateau, Bull. Geol. Soc. Am., 126, 1363–1383, https://doi.org/10.1130/B30983.1, 2014.

Riffel, S. B., Vasconcelos, P. M., Carmo, I. O., and Farley, K. A.: Goethite (U–Th)/He geochronology and precipitation mechanisms during weathering of basalts, Chem. Geol., 446, 18–32, https://doi.org/10.1016/j.chemgeo.2016.03.033, 2016.

Schultz, L. and Franke, L.: Helium, neon and argon in meteorites: A data collection, Meteorit. Planet. Sci., 39, 1889–1890, 2004.

Shukolyukov, Y. A., Yakubovich, O. V., Yakovleva, S. Z., Sal'nikova, E. B., Kotov, A. B., and Rytsk, E. Y.: Geothermochronology based on noble gases: III. Migration of radiogenic He in the crystal structure of native metals with applications to their isotopic dating, Petrology, 20, 1–20, https://doi.org/10.1134/S0869591112010043, 2012a.

Shukolyukov, Y. A., Yakubovich, O. V., Mochalov, A. G., Kotov, A. B., Sal'nikova, E. B., Yakovleva, S. Z., Korneev, S. I., and Gorokhovskii, B. M.: New geochronometer for the direct isotopic dating of native platinum minerals (190Pt-4He method), Petrology, 20, 491–505, https://doi.org/10.1134/S0869591112060033, 2012b.

Shuster, D. L. and Farley, K. A.: Diffusion kinetics of proton-induced He in quartz, Geochim. Cosmochim. Ac., 69, 2349–2359, https://doi.org/10.1016/j.gca.2004.11.002, 2005.

Shuster, D. L., Vasconcelos, P. M., Heim, J. A., and Farley, K. A.: Weathering geochronology by (U-Th) / He dating of goethite, Geochim. Cosmochim. Ac., 69, 659–673, https://doi.org/10.1016/j.gca.2004.07.028, 2005.

Strutt, R.: Helium and Radio-activity in Rare and Common Minerals, Proc. R. Soc. London. Ser. A, 80, 572–594, 1908.

Strutt, R.: The Accumulation o f Helium in Geological Time, Proc. R. Soc. London. Ser. A, 83, 298–301, 1909.

Stuart, F. M., Turner, G., Duckworth, R. C., and Fallick, A. E.: Helium isotopes as tracers of trapped hydrothermal fluids in ocean- floor sulfides, Geology, 22, 823–826, https://doi.org/10.1130/0091-7613(1994)022<0823:HIATOT>2.3.CO;2, 1994.

Vasconcelos, P. M., Heim, J. A., Farley, K. A., Monteiro, H., and Waltenberg, K.: 40Ar/39Ar and (U-Th) / He – 4He/3He geochronology of landscape evolution and channel iron deposit genesis at Lynn Peak, Western Australia, Geochim. Cosmochim. Ac., 117, 283–312, https://doi.org/10.1016/j.gca.2013.03.037, 2013.

Verhaert, M., Gautheron, C., Dekoninck, A., Vennemann, T., Pinna-Jamme, R., Mouttaqi, A., and Yans, J.: Unravelling the Temporal and Chemical Evolution of a Mineralizing Fluid in Karst-Hosted Deposits: A Record from Goethite in the High Atlas Foreland (Morocco), Minerals, 12, 1151, https://doi.org/10.3390/min12091151, 2022.

Vermeesch, P.: IsoplotR: A free and open toolbox for geochronology, Geosci. Front., 9, 1479–1493, https://doi.org/10.1016/j.gsf.2018.04.001, 2018.

Wernicke, R. S. and Lippolt, H. J.: Botryoidal hematite from the Schwarzwald (Germany) heterogeneous uranium distributions and their bearing on the helium dating method, EPSL, 114, 287–300, https://doi.org/10.1016/0012-821X(93)90031-4, 1993.

Wu, L. Y., Stuart, F. M., Di Nicola, L., Heizler, M., Benvenuti, M., and Hu, R. Z.: Multi-aliquot method for determining (U + Th)/He ages of hydrothermal hematite: Returning to Elba, Chem. Geol., 504, 151–157, https://doi.org/10.1016/j.chemgeo.2018.11.005, 2019.

Yakubovich, O.: New 190Pt-4He method of isotope geochronology for dating minerals of platinum, in: PhD thesis, Saint Petersburg University, St Petersburg, 126 pp., 2013 (in Russian).

Yakubovich, O., Podolskaya, M., Vikentyev, I., Fokina, E., and Kotov, A.: U-Th-He Geochronology of Pyrite from the Uzelga VMS Deposit (South Urals) – New Perspectives for Direct Dating of the Ore-Forming Processes, Minerals, 10, 1–20, https://doi.org/10.3390/min10070629, 2020.

Yakubovich, O. V., Shukolyukov, Y. A., Kotov, A. B., Brauns, M., Samsonov, A. V., Komarov, A. N., Yakovleva, S. Z., Sal'nikova, E. B., and Gorokhovskii, B. M.: U-Th-He dating of native gold: First results, problems, and outlooks, Petrology, 22, 429–437, https://doi.org/10.1134/S0869591114050075, 2014.

Yakubovich, O. V, Gedz, A. M., Vikentyev, I. V, Kotov, A. B., and Gorokhovskii, B. M.: Migration of Radiogenic Helium in the Crystal Structure of Sulfides and Prospects of Their Isotopic Dating, Petrology, 27, 59–78, https://doi.org/10.1134/S0869591118050089, 2019.

Yakubovich, O. V., Stuart, F. M., Ivanova, E. S., and Gervilla, F.: Constant 4He Concentration and 190Pt-4He age of Detrital Pt-Alloy Grains from the Santiago River, Ecuador: Potential as a 4He Mineral Reference Material, Geostand. Geoanalytical Res., 47, 957–968, https://doi.org/10.1111/ggr.12502, 2023.

Zhang, R., Jensen, L., Fitzsimmons, J., Sherrell, R. M., Lam, P., Xiang, Y., andJohn, S.: Iron isotope biogeochemical cycling in the Western Arctic Ocean, Global Biogeochem. Cy., 35, e2021GB006977, https://doi.org/10.1029/2021GB006977, 2021.